The interaction of C_6H_6 and C_6H_{12} with noble metal surfaces: Electronic level alignment and the origin of the interface dipole

Paul S. Bagus[a)]
Department of Chemistry, University of North Texas, Denton, Texas 76203–5070

Klaus Hermann[b)]
Fritz-Haber-Institut der Max-Planck-Gesselschaft, Faradayweg 4-6, 14195 Berlin, Germany

Christof Wöll[c)]
Lehrstuhl für Physikalische Chemie I, Ruhr-Universität Bochum, D-44780, Germany

(Received 25 July 2005; accepted 12 September 2005; published online 10 November 2005)

The electronic interaction of two molecules, the aromatic benzene (C_6H_6) and the saturated hydrocarbon cyclohexane (C_6H_{12}) with a Cu(111) surface, have been determined using precise, *ab initio* electronic structure calculations. For the interaction of these adsorbates with the substrate, we present a detailed analysis and decomposition of various individual chemical mechanisms that contribute. A novel aspect of this analysis is the use of charge-density difference contour plots to graphically display the chemistry. A wave-function-based approach was used in order to avoid problems when the presently most commonly employed approach, density-functional theory, is applied to weakly chemisorbed molecules, where the interaction is dominated by van der Waals forces. The present information are not only relevant with regard to understanding the chemistry going on when molecules are adsorbed on a Cu surface but also have important consequences with regard to charge injection in molecular electronic devices, e.g., organic field-effect transistors and organic light-emitting diodes. © *2005 American Institute of Physics*. [DOI: 10.1063/1.2107647]

I. INTRODUCTION

An important issue in molecular (or "plastic") electronics is the electronic level alignment at organic/metal interfaces. For an efficient electron injection, the Fermi level of the substrate and the energy of the lowest unoccupied molecular orbital (LUMO) must differ by a small amount of energy only. For hole injection, the same is true for the highest occupied molecular orbital (HOMO). Since for many of the organic molecule/metal combinations of interest precise calculations are not at hand, very often the so-called common vacuum level (CVL) approximation is used, see Fig. 1. In this simple model, which dates back to Mott[1] and Schottky,[2] positions of molecular electronic levels at the metal/organic interface are predicted by assuming that the vacuum level for the isolated systems, the metal and the free molecule, respectively, are simply aligned and by neglecting differential shifts between the different molecule orbitals. We have carried out *ab initio* wave-function-based electronic structure calculations to analyze the electronic structure at the interface of two hydrocarbons, benzene and cyclohexane, deposited on a copper surface. First, the calculations show that, although the adsorbate/substrate chemical interaction is weak in both cases, a significant change in the work function occurs. In previous work it has been realized that in many cases significant changes in the work function occur, which are not expected on the basis of the CVL. As a result, the concept of the interface dipole has been introduced, which proposes a uniform shift of all molecular electronic levels,[3,4] see Fig. 1. A major step towards understanding the physics responsible for the formation of the interface dipole has been made recently when by employing precise wave-function (WF)-based *ab initio* calculations the mechanism for interface-dipole formation in the simpler case of saturated hydrocarbons adsorbed on Cu could be identified.[5] In these calculations dispersion forces [commonly also referred to as van der Waals (vdW) forces] are considered explicitly and reliably by using Moller-Plesset second-order perturbation theory (MP2). It has been demonstrated that, in case of Cu, the origin of the unexpected, fairly strong interface dipoles is exchange repulsion.[5] This quantum-mechanical phenomenon, also referred to as *Pauli repulsion*, is always present but has, in the past, not been considered sufficiently large to explain the large changes in work function which are observed when chemically inert, closed-shell particles are physisorbed on the surface of a metal.

The objective of this paper is to examine and to interpret the characteristics of the bonding and interaction of adsorbed benzene and cyclohexane on a Cu surface, which is taken to be representative of noble metal surfaces. A novel aspect of our analysis involves our use of charge-density difference contour plots to permit a graphical display of individual contributions to the interaction. We also discuss certain aspects of the vibrational energies for frustrated translation of the adsorbate and, briefly, consider the calculated shifts of orbital energies of the adsorbate. A detailed understanding of these interactions and, in particular, of the differences between

[a)]Electronic mail: bagus@unt.edu
[b)]Electronic mail: hermann@fhi-berlin.mpg.de
[c)]Electronic mail: woell@pc.ruhr-uni-bochum.de

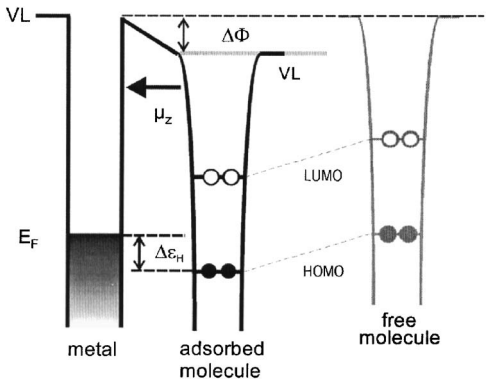

FIG. 1. Schematic representation of energy level positions at the metal/molecule interface. The standard model (right, gray), referred to as vacuum level alignment (VLA) is too simplistic; a realistic scheme has to take the interface dipole (μ_z) into account, which leads to a work-function change $\Delta\Phi$.

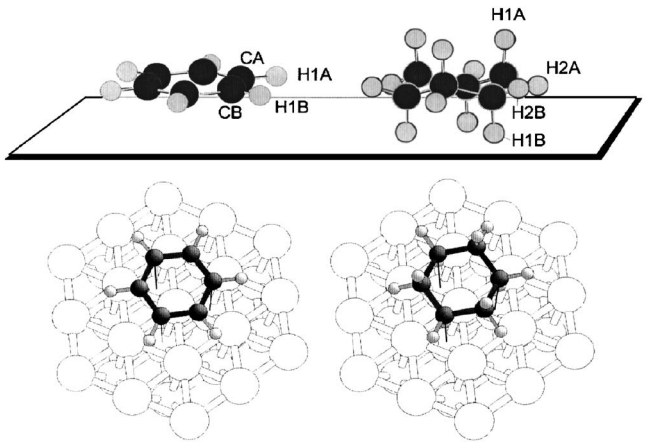

FIG. 2. Schematic representation and labeling for the hydrocarbon/Cu-cluster complexes studied here. CA is on a 3*h* site, CB on a fcc site.

benzene and cyclohexane will provide information useful to understanding how these and other organic adsorbates can affect the electronic properties of surfaces and interfaces. This understanding may also allow us to predict how such organic adsorbates might be used as components of molecular electronic devices. The theoretical analysis of the interaction is based on a constrained space orbital variation,[6,7] (CSOV) which permits the total bonding to be separated into contributions from the metal surface and from the molecular adsorbate. The CSOV also permits us to identify the consequences of the Pauli exclusion arising from the quantum-mechanical requirement that the total wave function of the system be antisymmetric.[5–7] The Pauli exclusion effects are identified by forming an antisymmetric wave function based on the superposition of the wave functions for the separated systems.[5] The contributions due the constrained variations of the orbitals of the metal substrate and of the organic adsorbate will be discussed in terms of polarization of each unit in the interaction and in terms of dative covalent bonding between the units. For the CSOV analysis, three properties of the constrained variation are considered: these are the energy at each CSOV step, the dipole moment at each CSOV step, and the difference of the charge densities going from one to another CSOV step. The energy and dipole moment have been treated rather commonly in the CSOV decomposition[5–7] to follow and quantify the chemical changes that take place as variational constraints are relaxed. The difference of the charge densities have not been used as extensively to identify the changes in charge density that are associated with the changes in other properties. As we show in the present work, these charge-density differences are useful tools to visualize the chemical changes associated with the various CSOV steps.

The principle results of our CSOV analysis are as follows. (1) The Pauli exclusion not only leads to a large steric repulsion but also to a large change in the interface dipole. This change in the dipole is in the direction of reducing the work function. Indeed, the change in the interface dipole because of the Pauli exclusion is larger than any of the other contributions to this dipole. (2) The changes, due to the variation of the Cu orbitals, arise principally from Cu polarization in response to the presence of the adsorbate and lead to a large reduction of the steric or Pauli, repulsion. (3) For C_6H_6 there is evidence for a weak dative covalent bond involving donation from the adsorbate into unoccupied orbitals of the substrate.

II. WAVE-FUNCTION METHODOLOGY AND CLUSTER MODELS

The molecular systems used to model the adsorbate-substrate interaction involved a 32 atom Cu cluster representing the unreconstructed and unrelaxed Cu(111) surface. This model contains 19 atoms in the first layer, 12 atoms in the second layer, and 1 atom in the third layer of Cu and is denoted Cu(19,12,1). The third layer atom, arbitrarily placed directly below the central first layer Cu atom, has been introduced primarily to allow us to treat the Cu_{32} and Cu_{32} plus an adsorbate as closed-shell systems. This is a significant convenience with certain of the computer programs that have been used. The seven atoms at the center of the first layer are treated with an 11-electron pseudopotential described as an effective core potential (ECP).[8] The remaining 25, environmental, atoms in the cluster are treated with a one-electron ECP.[9] The use of this one-electron ECP for the environmental atoms has been tested extensively and it has been found to permit substantial increase in the size of the cluster without introducing serious artifacts.[5,10,11] The molecular adsorbate is added so that the center of the C atoms is coincident with the central atom of the top layer of the cluster. The point-group symmetry of the Cu_{32} cluster model of Cu(111) is C_{3v}; the point-group symmetries of the adsorbates are reduced from the symmetry of the isolated adsorbates due to the interaction with the substrate and have, see below, C_{3v} symmetry. Thus, the symmetry of the total system of substrate and adsorbate, $Cu_{32}-X$, is C_{3v}. The cluster models and the adsorption site geometries are shown in Fig. 2. The wave functions for all systems considered are taken to be closed shell and they are ^1A states.

TABLE I. Optimized geometries for benzene and cyclohexane adsorbed in a planar adsorption geometry on the $Cu_{32}(19,12,1)$ cluster; gp indicates the gas-phase geometries. The atoms are labeled to indicate symmetry independent atoms; see Fig. 2 for a pictorial view of the adsorption geometry. CA is on a 3*h* site, CB on a fcc site.

	Cyclohexane			Benzene		
		CH bond length (Å)			CH bond length (Å)	
Atom	ΔS[a] (Å)	Adsorbed	gp	ΔS[a] (Å)	Adsorbed	gp
H1B	2.74	1.1016	1.0927	3.57	1.0871	1.0867
H2B	4.19	1.0978	1.0904			
H2A	3.92	1.0976	1.0904			
H1A	5.40	1.1006	1.0927	3.57	1.0875	1.0867
CA	3.84			3.58		
CB	4.30			3.60		

[a]ΔS denotes the distance to the surface in Å.

The geometry of the adsorbate has been optimized in order to determine the equilibrium distance of the molecule from the surface and the equilibrium geometry of the adsorbate in the presence of the Cu(111) substrate. The geometry optimization was performed using MP2.[12–14] We choose to use MP2 since MP2 provides a reasonably accurate representation of the vdW dispersion forces that provide the major part of the bonding interaction in these weakly bound systems.[5,15] Although the coupled cluster (CC) theory may provide a somewhat more accurate treatment of the vdW interaction,[16] the additional computational demands of the CC calculations would have limited our ability to treat the large Cu clusters necessary to properly model the C_6H_6 and C_6H_{12} interactions with Cu(111). We have avoided using density-functional theory (DFT) because of the difficulties encountered treating the vdW systems with DFT.[5,16–18] In particular, we recall that the bond strength determined for systems where vdW dispersion forces make major contributions depends very strongly on the particular functional used for the DFT calculations. The choice of an appropriate functional to obtain reliable bond strengths is not at all clear. For these MP2 calculations, we have included the so-called counterpoise "corrections" due to basis-set superposition effects (BSSEs) using the procedure originally proposed by Boys and Bernardi.[19] This is done because our concern with the MP2 calculations is to obtain reliable equilibrium geometries. Neglecting the BSSE corrections, especially for weak interactions where vdW forces dominate, will yield bond distances that are much too small and bond depths that are much too deep.[19,20] Large basis sets of size 6-311++G** were used for the C and H atoms. For the 11-electron ECP Cu atoms, the basis set given by Hay and Wadt[8] augmented with diffuse *s* and *p* functions to represent the Cu "conduction-band" charge density were used; for the one-electron ECP Cu atoms, a similarly augmented basis set, described in Ref. 5, was used. In the MP2 calculations, the *s* combinations of the Cartesian *d* basis functions were not included.

For both molecules, the geometry was optimized using the MOLPRO program package.[21] Only the coordinates of the atoms within the hydrocarbon molecule were optimized; the positions of the copper atoms were kept fixed at their bulk positions. In effect, we have not allowed the surface Cu atoms to relax or reconstruct. We have used this simplification of the geometry optimization because the main focus of our interest is for the global features of the adsorbate-substrate interaction, which we believe are not significantly modified by the surface relaxation. In this connection, we recall that we have used a similarly frozen substrate geometry in our previous study of the lateral vibrations of CO/Cu(100).[22] Despite the fact that CO has a much stronger interaction with a Cu surface than either benzene or cyclohexane, we were able to obtain *quantitative* agreement between the experimental and theoretical data regarding the CO vibrational modes with our model of a frozen, unrelaxed Cu surface. This result gives strong support to our choice to neglect optimization of the positions of the Cu atoms and indicates that any changes resulting from such an optimization are very likely to be minor. During the geometry optimization, the symmetry was fixed to be C_{3V}. The most important difference of the present work with previous calculations carried out for these systems[15,23] is that the optimization was carried out with the BSSE corrections of the gradients, instead of only correcting the energy of the final geometry obtained from an optimization without the BSSE correction. The corresponding geometries are shown in Fig. 2 for both benzene and cyclohexane; the numerical values are tabulated in Table I. It is noteworthy that, in both cases, the deviation from the gas-phase geometry is very small. For cyclohexane this result is—in view of the previous results obtained for this and the smaller saturated hydrocarbons propane and cyclopropane[15,23]—not surprising. For benzene on Cu(100), previous DFT calculations have suggested that the geometry changes are very small.[24] We would like to point out, however, that for the related case of benzene adsorbed on the more open Cu(110) surface a quite substantial adsorption-induced intramolecular distortion has been observed.[24] The binding energy of C_6H_{12} to the Cu substrate for the optimized geometry amounted to 307 meV, that for C_6H_6 to 350 meV. Both values were corrected for the BSSE effects. These theoretical values are significantly smaller than the experimental values of 470 meV for cyclohexane/Cu(111) (Ref. 25) and of 590 meV for C_6H_6/Cu(111)

(Ref. 26 and 27). These differences are similar to that seen in previous work[5,15,23] and are attributed to the finite size of the Cu cluster used in the present calculations.

At the equilibrium geometry determined by the MP2 calculations, a CSOV analysis[6,7] was carried out with Hartree-Fock (HF) wave functions (WFs). The HF WFs do not include dispersion forces and, hence, do not fully describe the bond energy. However, they do properly include the major chemical changes that occur within and between the substrate and adsorbate subunits; these chemical changes include both polarization effects and the chemical bonding that may occur between these subunits. While vdW dispersion forces do lead to changes in the charge density of the system, one can argue that these changes are relatively small. This argument involves the weak forces on the adsorbates due to the vdW interactions. These forces are responsible for the vibrational energies of the frustrated translation of the adsorbates normal to the surface and, as discussed in Sec. III, the energies for these translations are quite small, $\sim 50\ \mathrm{cm}^{-1}$. The Hellman-Feynman theorem[28] relates the forces and, hence, the force constants[29] to integrals over the electron density ρ. Since the vibrational frequencies are quite small, we can reasonably anticipate that the vdW-induced changes in ρ are also small. Furthermore, the vdW interaction is viewed in physical terms as an induced dipole-induced dipole interaction.[30] The vdW interaction at a surface is amplified over that between individual atoms or molecules because of the summation over many substrate atoms; however, the individual-induced dipoles both in the surface and in the adsorbate may not be especially large. In any event, as we show in Sec. IV, the chemistry at the HF level leads to significant changes that need to be understood. The CSOV decomposition of the HF WFs gives a major enhancement and refinement of our understanding of the chemical bonding interactions and of the consequences of these chemical changes for other properties. These properties include the interface dipole,[5] shifts of the vibrational frequencies of adsorbed molecules,[31,32] and binding energy shifts as observed in photoemission.[10,33] In addition, we note that while it is possible to apply a CSOV analysis to correlated multiconfiguration WFs,[34] it is not clear that such an analysis is useful for the interpretation of weak, vdW, dispersion forces. The essence of a CSOV analysis is the decomposition of an interaction to determine the separate contributions from each of the partners in the interaction. On the other hand, the vdW contribution to the interaction arises from an induced dipole-induced dipole term[30] that is a coupled, simultaneous, contribution from both partners, which is outside the conceptual framework of the CSOV analysis.

The four CSOV steps used to decompose the interaction, frozen orbital (FO), vary Cu substrate $[V(\mathrm{Cu})]$, vary adsorbate $[V(\mathrm{adsorbate})]$, and full self-consistent field (SCF) are described below. However, before we turn to a discussion of the essential features of the individual CSOV steps, we wish to stress that the computations for each of the CSOV steps involve the SCF solution of a Fock matrix where appropriate variational constraints are imposed on the matrix elements.[6,7] Thus, at each of the CSOV steps as well as at the total, unconstrained full SCF step, one obtains total and orbital energies and other properties of the WFs. Next, we consider, in turn, the constraints imposed on each of the four CSOV steps. The FO step involves forming an antisymmetric wave function for the combination of adsorbate and substrate by combining the fixed, or frozen, orbitals of the two components. No chemical changes are permitted at this step, hence the name FO. In the second, $V(\mathrm{Cu})$, CSOV step, the orbitals of the adsorbate are fixed but the Cu orbitals are varied so that they can respond to the presence of the adsorbate. In principle, this step includes both polarization of the Cu substrate to reduce the steric or Pauli repulsion with the adsorbate and, also, dative covalent bonding, donation, from substrate to adsorbate. In the third, $V(\mathrm{adsorbate})$, CSOV step, the Cu orbitals are fixed as they were obtained in the preceeding step, $V(\mathrm{Cu})$, and the adsorbate orbitals are varied to account for the presence of the substrate. As for $V(\mathrm{Cu})$, this step also, in principle, contains the effects of adsorbate polarization and adsorbate back donation to the substrate. The final step, full SCF, is a free, unconstrained variation of all the orbitals. Any changes at this step represent a nonadditivity of the separated variations in the $V(\mathrm{Cu})$ and $V(\mathrm{adsorbate})$ steps. Small changes between the $V(\mathrm{adsorbate})$ and full SCF steps indicate that the CSOV decomposition is reliable. In the $V(\mathrm{Cu})$ and $V(\mathrm{adsorbate})$ steps, we chose not to try to separate donations from polarization effects by dividing the virtual orbital space into orbitals "localized" on different centers.[6,7] This was done because we noted that there were artifacts arising from BSSE;[15] this was especially true since the adsorbate basis functions were able to represent, in part, polarizations of Cu(111) due to the presence of the adsorbate. Thus for the distinction between polarization and donation, leading to the formation of dative covalent bonds, we rely on the chemical properties of the subunits as electron acceptors or donors. In particular, we recall that neither C_6H_6 nor C_6H_{12} are normally able to accept charge from an electron donor. For the CSOV calculations, the same basis sets and ECPs for the Cu atoms were used as for the MP2 calculations described above. For the C and H atoms, a large basis set including diffuse functions was used. These basis sets are similar to those used in our earlier work for the adsorption of C_3H_8 on Cu(111).[11]

III. ADSORBATE VIBRATIONS

Although a complete normal-mode analysis of the present adsorbate/substrate complex (see Refs. 15 and 23) was not possible because of the large size of the adsorbate/cluster complex, we have determined the energy of the frustrated translation of the absorbed molecule normal to the surface. The exact procedure was as follows. Using the optimized adsorbate geometry, determined as described above, we obtained a one-dimensional potential-energy curve by moving the adsorbate with respect to the surface. For this potential curve, the intramolecular geometry was fixed as obtained from the full optimization. In effect, we are separating the frustrated translation of the adsorbate from the intramolecular vibrations of the adsorbate. If the frequency of the frustrated translation is sufficiently different from the

TABLE II. CSOV decomposition for the C_6H_6–Cu(111) interaction as modeled with the $Cu_{32}C_6H_6$ cluster. The interaction energy E_{INT} and ΔE_{INT} are in eV and the z component of the dipole moment μ, as well as $\Delta\mu$ are given in Debye. See the text for a detailed description of the information presented.

CSOV step	$E_{INT}/\Delta E_{INT}$	$\mu/\Delta\mu$
$\mu(C_6H_6)$	···	−0.07
$\mu(Cu_{32})$	···	−2.05
μ_{ref}	···	−2.12
FO	−0.48/···	−1.20/+0.92
V(Cu)	−0.09/+0.39	−1.14/+0.06
$V(C_6H_6)$	−0.04/+0.05	−0.78/+0.37
Full SCF-nonadditive	−0.04/+0.00	−0.72/+0.06
Total $\Delta\mu$	···	···/+1.40

intramolecular modes with which it is symmetry allowed to couple, this approximation will give reliable values for the frustrated translation.[35] With this one-dimensional potential curve, the harmonic vibrational frequency ω_e for the frustrated vibration was determined using a Dunham analysis.[36] For ω_e, the positions of Cu substrate atoms were kept fixed; hence the adsorbate motion was decoupled from the surface phonons; this has been found to be an excellent approximation for the vibrations of CO on a Cu surface.[22,32,35] We expect this decoupling of molecular vibrations from the surface phonons to hold generally. The Dunham analysis was carried out using six or seven C_6H_6 positions in a region of ~1 Å about the equilibrium distance of the adsorbate from the surface. The Dunham analysis depends on a polynomial fit to the potential curve and we used both cubic and quartic polynomials for this fit. We found very small differences in the ω_e, ~0.2 cm^{-1}, obtained with these two polynomials and this establishes the reliability of our fits. For C_6H_6, ω_e = 51 cm^{-1} and for C_6H_{12}, ω_e = 37 cm^{-1}. The slightly larger mass of C_6H_{12} compared to C_6H_6 would only account for an ~4% reduction of ω_e for C_6H_{12}. Thus the decrease of ω_e for C_6H_{12} arises from differences in the potential curves for these two adsorbates and it suggests a weaker bonding for C_6H_{12}/Cu than for C_6H_6/Cu. This is consistent with our results, see below, that the vdW physisorption bond is in the case of C_6H_6 augmented by a weak π donation from C_6H_6 to the Cu surface.

Unfortunately, there is no experimental data available for the frustrated translation of benzene or cyclohexane normal to the Cu(111) surface, but the corresponding frequencies have been determined for the rather similar case of Cu(100) substrates. Here the energy of the frustrated translational vibration amounts to 7.3 meV ≈ 59 cm^{-1} for both, cyclohexane and benzene.[37] This energy compares rather well with the theoretical values determined here, especially for benzene while the energy observed for C_6H_{12} is somewhat larger than our calculated value. The fact that the vibrational energy for cyclohexane adsorbed on Cu(100) is almost the same than for benzene suggests that on the Cu(100) surface the interaction between cyclohexane and the Cu surface is stronger than in the present case of Cu(111).

TABLE III. CSOV decomposition for the C_6H_{12}–Cu(111) interaction as modeled with the $Cu_{32}C_6H_{12}$ cluster; see caption to Table II.

CSOV step	$E_{INT}/\Delta E_{INT}$	$\mu/\Delta\mu$
$\mu(C_6H_{12})$	···	−0.01
$\mu(Cu_{32})$	···	−2.05
μ_{ref}	···	−2.05
FO	−0.41/···	−1.19/+0.87
V(Cu)	+0.00/+0.41	−1.40/−0.21
$V(C_6H_{12})$	+0.04/+0.04	−1.35/+0.05
Full SCF-nonadditive	+0.04/+0.00	−1.38/−0.04
Total $\Delta\mu$	···	···/+0.67

IV. CSOV ANALYSES AND THE CHARACTER OF THE INTERACTION

A. Tabulated and graphical Data from the CSOV analysis

For both adsorbate systems,denoted Cu_{32}–X, the interaction energy E_{INT} is computed at each step of the CSOV analysis; these interaction energies, $E_{INT}(Cu_{32}–X;$ CSOV step), are defined as the difference of the energy of the complex and the sum of the energies of the separated subunits:

$$E_{INT}(Cu_{32}-X;\text{CSOV step } n) = [E(Cu_{32})+E(X)] - E(Cu_{32}-X;\text{CSOV step } n). \quad (1)$$

The change of the energy at each step from that of the preceding step, denoted ΔE_{INT}, indicates the importance of the newly allowed variational freedom for the energetics of the interaction. In a similar way, the changes in the dipole moment μ are analyzed. Given the C_{3v} point-group symmetry, the only nonzero component of μ is along the direction normal to the surface, which is taken to be the z axis. However, although we give only values of μ_z, they are referred to simply as μ. The sum of the dipole moments of the separated subunits is taken as the reference of the dipole moment,

$$\mu_{ref}(Cu_{32}-X) = \mu(Cu_{32}) + \mu(X). \quad (2)$$

For each of the CSOV steps, the change in the dipole moment $\Delta\mu$ is given as a measure of the direction and the magnitude of the motion of charge;

$$\Delta\mu(Cu_{32}-X;\text{CSOV step } n) = \mu(Cu_{32}-X;\text{CSOV step } n) - \mu(Cu_{32}-X;\text{CSOV step } n-1). \quad (3)$$

For the FO first step of the CSOV, the difference $\Delta\mu$ is taken with respect to μ_{ref}, see Eq. (2). The sign of $\Delta\mu$ is such that $\Delta\mu<0$ corresponds to a motion of the center of electronic charge to larger values of z or in a direction towards above the Cu(111) surface, while $\Delta\mu>0$ corresponds to a motion of the center of charge towards below the surface. It is worth noting that the motion of charge may not be uniform but it may move above the surface in certain regions of space and below the surface in other regions. Thus, a small value of $|\Delta\mu|$ does not necessarily mean that there is very little net motion of charge;rather,the small $|\Delta\mu|$ may arise because there are canceling contributions to $\Delta\mu$ from different

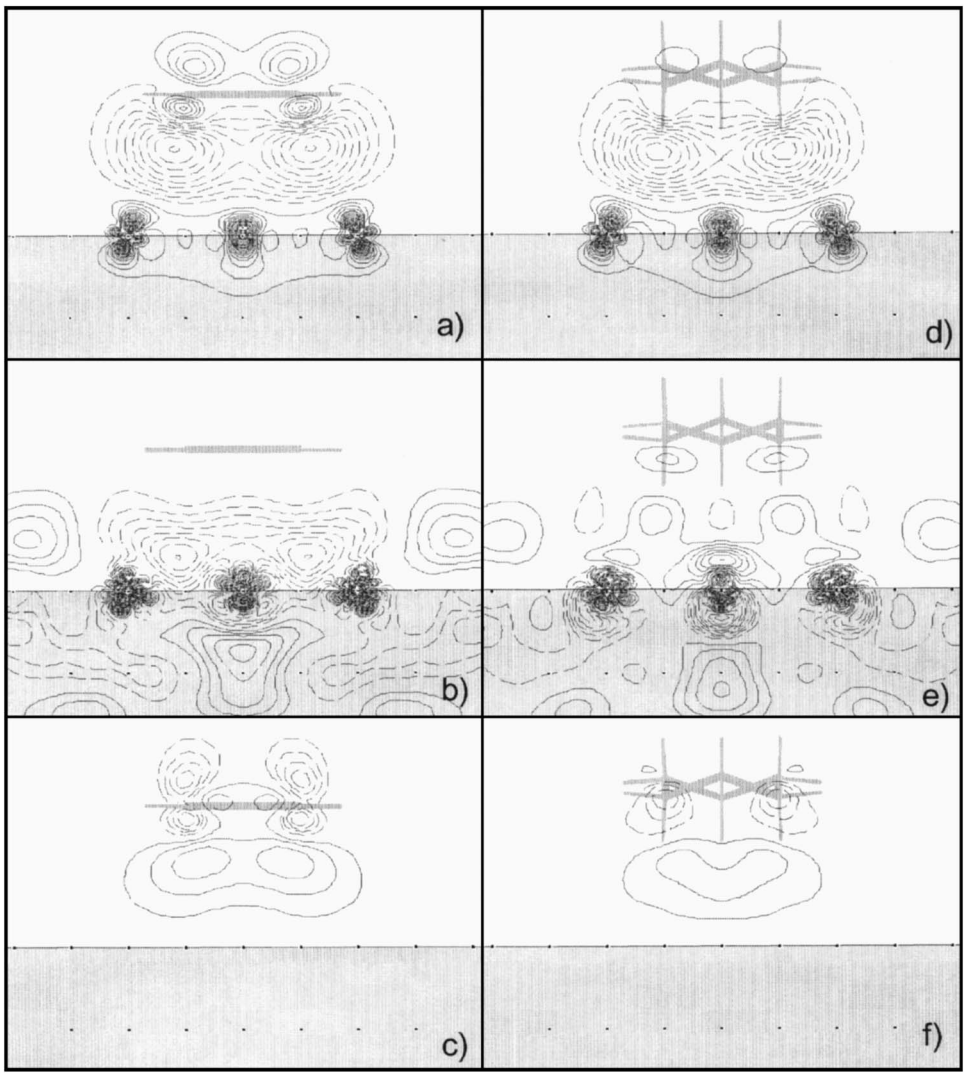

FIG. 3. Charge-density difference contours for various CSOV steps in the decomposition of the interaction for $C_6H_6/Cu(111)$ [(a)–(c)] and for $C_6H_{12}/Cu(111)$ [(d)–(f)]. The y axes of the plot planes are along the normal to the Cu surface; the positions of the atoms with respect to the surface are indicated on the figures. The solid lines are contours for $\Delta\rho>0$ while the dashed lines are contours for $\Delta\rho<0$; see the text for more information about the parameters used in these plots. (a) and (d) are the differences, of the FO density minus the sum of the densities of the adsorbate and substrate, Eq. (4a). (b) and (e) are the differences of the density at the V(Cu) CSOV step minus the FO density, Eq. (4b). (c) and (f) are the differences of the density at the V(adsorbate) CSOV step minus the V(Cu) density, Eq. (4c).

regions. This cancelation has been observed at the V(Cu) CSOV step for Xe/Cu(111) (Ref. 5) where Cu charge directly below the Xe atom is pushed down below the surface while Cu charge at the periphery of the Xe atom moves above the surface. Indeed, a similar behavior is seen for the systems considered in the present study.

The CSOV values for E_{INT}, ΔE_{INT}, μ, and $\Delta\mu$ for $C_6H_6/Cu(111)$ and for $C_6H_{12}/Cu(111)$ are given in Tables II and III, respectively. The values of μ for the cluster model of Cu(111), $\mu(Cu_{32})$, for the isolated adsorbate, $\mu(X)$, and for their sum μ_{ref}, see Eq. (2), are also given in the tables; in addition the total change in μ, denoted Total $\Delta\mu$, from μ_{ref} to μ (full SCF) is also given. The values given in Tables II and III do not include estimates of the effects due to BSSE since our concern is for the qualitative nature of the CSOV changes. However, we have confirmed both for similar systems[11] and for the present systems that the BSSE effects are small for the WF calculations at the HF level.

In order to gain detailed insight into how the motion of charge may vary in different regions of space, we present contour plots of charge-density differences, $\Delta\rho$, in Figs. 3 and 4; the $\Delta\rho$ are taken between the various CSOV steps. The four $\Delta\rho$ plots that are reported are specifically for

$$\Delta\rho(Cu_{32}-X;\mathrm{FO})=\rho(Cu_{32}-X;\mathrm{FO})-[\rho(Cu_{32})+\rho(X)], \tag{4a}$$

$$\Delta\rho(Cu_{32}-X,V(Cu))=\rho(Cu_{32}-X;V(Cu))-\rho(Cu_{32}-X;\mathrm{FO}), \tag{4b}$$

$$\Delta\rho(Cu_{32}-X,V(X))=\rho(Cu_{32}-X;V(X))-\rho(Cu_{32}-X;V(Cu)),\ \text{and} \tag{4c}$$

$$\Delta\rho(Cu_{32}-X,\text{full SCF})=\rho(Cu_{32}-X;\text{full SCF})-[\rho(Cu_{32})+\rho(X)]. \tag{4d}$$

The ρ for the various CSOV WF are defined in the usual way for antisymmetrized HF WFs.[38] The contour plots of $\Delta\rho$ are made for a given plane. The plane chosen for our plots is perpendicular to the surface and passes through the central Cu atom of the Cu_{32} cluster and through two of the six nearest-neighbor Cu atoms in the first surface layer. The plotting plane also passes through the centers of the two triangles of C atoms in the C_{3V} optimized geometry of the C_6H_6 and C_6H_{12} adsorbates; it is parallel to the bases of the triangles and none of the C or H atoms is in the plotting plane. The x

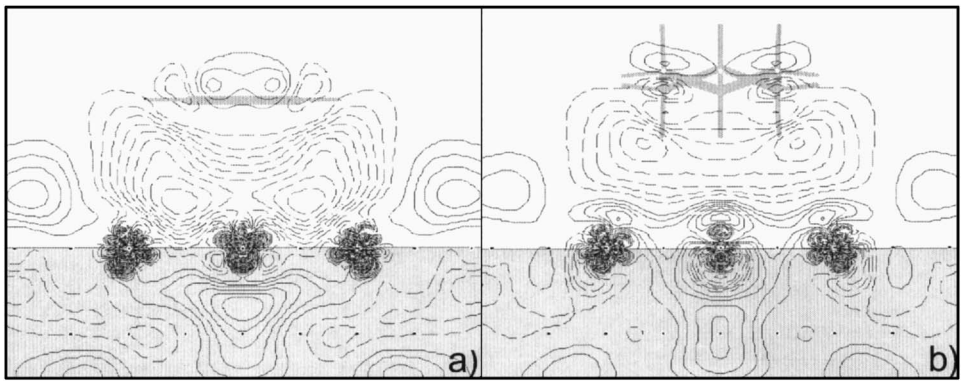

FIG. 4. Charge-density difference contours for the total adsorbate-substrate interactions for C_6H_6/Cu(111) (a) and for C_6H_{12}/Cu(111) (b). The plots are for the density of the full SCF WF minus the sum of the densities of the adsorbate and substrate. See the caption to Fig. 3 and the text for further information about the contours and the plotting plane.

axis of the plot measures distance along the surface and the y axis of the plot measures distance normal to the surface. See Fig. 2 for a pictorial representation of the adsorbate-substrate clusters and as a guide to the choice of plotting plane for the plots. For all the plots, the x axis extends from $-5.3\ \text{Å} \leqslant x \leqslant +5.3\ \text{Å}$ and the y axis extends from $-3.2\ \text{Å} \leqslant y \leqslant +5.8\ \text{Å}$. The contours for constant $\Delta\rho$ are shown as solid lines for $\Delta\rho > 0$ and they are shown as dashed lines for $\Delta\rho < 0$. The difference between consecutive contours of $\Delta\rho$ is 0.0005 electrons/(bohr)^3. Although there is a cutoff for large $|\Delta\rho|$, regions very near atoms in the plane appear black because of the large number of contours in this region.

The density difference plots for Eqs. (4a)–(4c) are given for C_6H_6/Cu(111) in Figs. 3(a)–3(c), and for C_6H_{12}/Cu(111) in Figs. 3(d)–3(f); the plots for Eq. (4d) are given in Fig. 4. The two rows of dots in the figures indicate the position, with respect to the plotting plane, of the surface Cu atoms and the atoms in the second Cu layer. The region of the Cu substrate is shown as shaded to distinguish it from the region above the interface. The Cu atom in the third layer is not shown but, from the data in the figures, it is clear that the influence of the adsorbates is predominately in and around the surface Cu layer, although the polarization of the Cu atoms extends to the second Cu layer, see Figs. 3(b) and 3(e). In the first Cu layer three atomic centers are in the plane of the plot; these are the central atom and the second nearest neighbors to the left and the right of the center. These atoms are identified, in Figs. 3(a), 3(b), 3(d), and 3(e), by the large density changes in the immediate region of the atomic centers. The position of the adsorbate, with respect to the plotting plane, is indicated schematically, in Figs. 3 and 4, by the sketched shading above the Cu surface. The thicker lines are used to connect C atoms to each other and the thinner lines are used to connect each C atom to the nearest H atom; although for C_6H_6, the C–H bonds perpendicular to the plotting plane cannot be shown. The distortion of C_6H_6 from planarity is quite small and cannot be seen in the sketch of this molecule. All the C and H atoms of C_6H_6 are ~3.6 Å above the surface and differ in height by only ~0.02 Å. The situation is somewhat more complex for the more three-dimensional C_6H_{12} molecule, see Fig. 2. For C_6H_{12}/Cu(111), the C and H atoms occupy six distinct rows ranging from 3.9 to 5.4 Å above the first layer Cu atoms. Each of these rows contains either three H atoms or three C atoms with, depending on the row, either two atoms above and one atom below the plotting plane or two below and one above this plane. By combining the molecular sketches in Figs. 3 and 4 with the models shown in Fig. 2, one can identify the positions of the adsorbate atoms with respect to the plotting plane.

B. CSOV decomposition of the adsorbate-substrate interaction

1. CSOV step 1: Frozen orbitals

We consider first the FO CSOV step where an antisymmetric wave function is formed from the superposition of the WFs for the separated substrate and adsorbate systems. Thus, at this step, only the Pauli exclusion principle, or the so-called Pauli or steric repulsion, is taken into account. Tables II and III show that there is a substantial, although similar, steric repulsion between the adsorbates and the Cu(111) substrate. The FO repulsion energy is 0.5 eV for C_6H_6/Cu(111) and 0.4 eV for C_6H_{12}/Cu(111) and is entirely expected.[11,39] There is also a rather large change in the surface or interface dipole of +0.9 D for both adsorbates. This change in the interface dipole arises entirely from the Pauli exclusion principle[5] and this is very clearly shown in Figs. 3(a) and 3(d). The Pauli exclusion principle states that electrons of the same spin do not want to be in the same region of space. The large number of dashed contours in the region between the surface and the adsorbate in these figures shows the depletion of charge between the units. This depletion arises because the orbitals of the adsorbate and substrate overlap.[5] There is also, as required by the Pauli exclusion principle, an increase of charge density around the absorbate and substrate as shown by the full line contours in Figs. 3(a) and 3(d). However, the increase of charge density is not equal about the adsorbate and substrate. It is much greater at the substrate than at the adsorbate; see the much larger number of contours around the first layer Cu atoms than near the atoms of the adsorbate. However, from the contour plots of Figs. 3(a) and 3(d), it is not possible to quantify how large is the increase of charge density at the substrate since this requires an integration of $\Delta\rho$ over all space. On the other hand, this integration of $\Delta\rho$ is precisely the information contained in the values of $\Delta\mu$.[5] Clearly, see Tables II and III, there is a major net motion of charge from the adsorbate toward the substrate. We have observed that the net motion of charge due to the Pauli exclusion principle is in the direction of the more polarizable subunit where there is a larger amount of diffuse charge. The substrate is more polarizable than the

relatively electronically rigid adsorbates and the motion of the center of charge toward the substrate due simply to forming an antisymmetric WF for the total, adsorbate+substrate, system is large. This change occurs simply to satisfy the requirement of the Pauli exclusion principle.

2. CSOV step 2: Substrate polarization

The second CSOV step, V(Cu), includes, in principle, both polarization of the Cu charge density as well as back donation from occupied Cu orbitals. However, neither C_6H_6 nor C_6H_{12} are good electron acceptors and the major, if not the entire, contributions at the V(Cu) CSOV step arise because of the polarization of the Cu charge. This will become clear when we examine the density difference contours in Figs. 3(b) and 3(e). The behavior of the Cu polarization is somewhat different for C_6H_6 and C_6H_{12} and we will discuss the results for C_6H_6, presented in Table II and Fig. 3(b) first. The polarization of the Cu charge reduces the steric repulsion by 0.4 eV. We caution that a small portion of this decrease in the repulsion is due to BSSE, although it is difficult to use the Boys-Bernardi counterpoise correction[19] to estimate the magnitude of the BSSE.[15] This is because the basis-set requirements for the polarized Cu surface in the presence of C_6H_6 are different from those for the isolated surface. We defer discussion of these different basis-set requirements and consider them below.

We point out that the magnitude of the change in μ at V(Cu) for C_6H_6/Cu(111) is rather small, being only 0.06 D, especially considering the relatively large change in E_{INT}. The charge-density difference contours in Fig. 3(b) explain why $\Delta\mu$ is quite small. The Cu charge directly below C_6H_6 is substantially reduced and this reduces the large steric repulsion. A critical question, however, is where the charge that had been between Cu(111) and C_6H_6 goes. This can also be seen from Fig. 3(b) and the result is somewhat surprising. A portion of the charge removed from the region between Cu and C_6H_6 goes below the first layer Cu atom at the center of the adsorbate as can be seen by the solid line contours in Fig. 3(b) below this atom. The reduction of Cu charge above the surface and the increase of charge below the surface should lead to a significant increase in μ; however, there is a compensating effect that reduces the change in μ. There are solid contours indicating an increase of Cu charge at the periphery of the C_6H_6 adsorbate; this motion of charge above the surface acts to reduce the increase in μ and leads to a small net $\Delta\mu$. This motion of substrate charge upwards will not increase the Pauli repulsion with the adsorbate since the adsorbate charge density is very small in the region where the substrate charge moves upward, see Fig. 2. The compensating motion of charge for the Cu polarization also occurs when Xe is adsorbed on Cu(111).[5] Furthermore, we show below that a similar effect occurs for C_6H_{12}/Cu(111).

A driving force for this compensation may be that it reduces the overall change in the interface dipole or, equivalently, in the global surface work function. For the cases of Xe (Ref. 5) and C_6H_6 on a metal surface, it may well be appropriate to characterize the polarization of the substrate charge as forming a sort of coffee cup where the charge goes below the surface directly beneath the adsorbate and it moves above the surface at the edges, or periphery, of the adsorbate. While this analog appears to be appropriate for the adsorption of weakly bound C_6H_6 and Xe, the results for C_6H_{12}/Cu, see below, show that the analog of a coffee cup is, in certain cases, an oversimplification. A final point shown by Fig. 3(b) is that there is no significant back donation from Cu to the unoccupied orbitals of C_6H_6. If there were such a back donation,[40] then there would be solid contours showing an increase of charge between the surface and the adsorbate. The chemistry of a covalent bond is that it builds up charge between the subunits that are bonded. Clearly this buildup of charge does not occur between Cu and C_6H_6. In fact, the changes of the Cu charge density go to zero $\sim$1–1.5 Å before the position of the C and H atoms in the C_6H_6. Figure 3(b) shows that the charge redistribution at the V(Cu) CSOV step is simply a polarization of the Cu charge, exactly as we had expected.

For C_6H_{12}/Cu(111), the V(Cu) CSOV step, see Table III, also leads to a 0.4 eV reduction in the steric repulsion; for reasons that we explain below, we believe that the BSSE contribution to the change in E_{INT} is larger for the adsorption of C_6H_{12} on Cu(111) than for the case of C_6H_6. Following our arguments above, the dominant origin of the reduction of the steric repulsion is the polarization of the Cu charge to avoid overlap with the charge of the C_6H_{12} adsorbate. However, the $\Delta\mu$ at this CSOV step is quite different from that for C_6H_6/Cu; in this case, the $\Delta\mu$=−0.2 D is much larger in magnitude than for C_6H_6 and the negative sign for $\Delta\mu$ indicates that the overall direction of the motion of the Cu charge is upward toward the C_6H_{12}. While this would appear to indicate the formation of a covalent bond by back donation from Cu to C_6H_{12}, the charge-density differences in Fig. 3(e) show that the increase in μ is due to a more complex polarization of the Cu charge than was the case for C_6H_6/Cu(111). The polarization is more complex largely because C_6H_{12} has a more open structure than C_6H_6. There is a decrease of charge immediately around the three Cu atoms in the plane of the plot and there is also an increase of charge shown by the solid contours below the Cu surface, especially directly below the central atom of the first layer. These changes contribute to an increase in μ. However, there are also increases in ρ above the first layer atoms of the Cu surface. The solid contours beyond the left and right edges of the C_6H_{12} adsorbate indicate increases of charge at the periphery of the adsorbate and are similar to the increase seen above the surface. The increase of the Cu charge density in this peripheral region is smaller for C_6H_{12} than was found for C_6H_6; compare Figs. 3(b) and 3(e). However, for the C_6H_{12} adsorbate, there is a large increase of Cu charge above the Cu surface directly below the first row of H atoms from the adsorbate. This might appear to be a back donation from Cu to C_6H_{12} indicating the formation of a covalent bond until it is recalled that the three H atoms in this row are not in the plane of the contour plot. The edge H atoms are 0.8 Å above the plotting plane and the center H atom is 1.5 Å below the plane. Thus, the increases in Cu charge density above the surface are not directed toward the H atoms but are in regions of space between the H atoms. This charge does not indicate a back donation but, rather, it is simply polarization

of Cu charge into empty spaces in the relatively open geometric structure of C_6H_{12}. There are also two regions where there is a charge increase between the first row of H and the first row of C atoms of C_6H_{12}; these increases might be viewed as indicating a Cu back donation to C_6H_{12}. However, each region has a small area and contains only two contours; thus the increase of charge in this region is quite small. It is likely that this small increase is an artifact related to the orthogonalization of the Cu orbitals to the occupied C_6H_{12} orbitals and we do not consider it further. The net effect of the polarization of Cu charge into the open spaces between the lowest row of H atoms in C_6H_{12} leads to a modest decrease of the interface dipole, $\Delta\mu=-0.2$ D, that offsets the increase in μ at the FO charge superposition CSOV step. This cancelation suggests that the work-function change induced by C_6H_{12} adsorbed on Cu(111) will be less than that induced by C_6H_6, which is consistent with observations.[41] However, we postpone a comparison with experiment until after we analyze the contributions of the CSOV steps where the adsorbate orbitals are varied, $V(C_6H_6)$ and $V(C_6H_{12})$. At this point, we do note that the reduction of the work function induced by a weakly bound adsorbate where dispersion forces dominate to determine the adsorbate-surface bond will be affected by whether the geometric structure of the molecule is relatively compact, as for C_6H_6 or relatively open, as for C_6H_{12}.

3. CSOV step 3: Molecule polarization

The third CSOV steps, $V(C_6H_6)$ and $V(C_6H_{12})$, involve variation of the adsorbate orbitals in the presence of the fixed charge density of the Cu substrate. For both adsorbates, the change in E_{INT} at this CSOV step is small, $\Delta E_{INT} \approx +0.05$ eV, indicating that the polarization of the adsorbate and the donation from the adsorbate are small and do not contribute significantly to the bonding of the adsorbates to the Cu surface. However, the $\Delta\mu$ at this CSOV step are different for the two adsorbates. For C_6H_6, $\Delta\mu=+0.4$ D; this positive change in μ is consistent with a donation from the higher-lying orbitals of C_6H_6 to unoccupied Cu surface conduction-band orbitals to form a dative covalent bond. The charge-density difference plot for the $V(C_6H_6)$ CSOV step, Fig. 3(c), clearly shows the formation of this dative covalent bond. There is an increase of charge between the row of C and H atoms and the first layer Cu surface atoms. There is also a decrease of charge about two of the C atoms; from the shape of the dashed contours, the decrease of charge is from C_6H_6 p_z or π orbitals, which are the high-lying orbitals of C_6H_6. These are precisely the orbitals that would be expected to be involved in donation from C_6H_6. Thus the overall picture is of a weak chemical bond forming by π donation in addition to the polarization of the Cu surface charge to reduce the steric repulsion. The change in μ of +0.4 D acts to further increase the change in the interface dipole in a direction that lowers the work function. For C_6H_{12}/Cu(111), $\Delta\mu=+0.05$ D suggesting an even weaker chemical bond than for C_6H_6, if, indeed, there is a chemical bond at all. The charge-density difference contours in Fig. 3(f) indicate that there is a small depletion of charge about the first row of C atoms above the Cu surface and a small increase of charge between the C_6H_{12} and the surface. However, it is easy to see by comparing Figs. 3(c) and 3(f) that the π donation from C_6H_{12} to the Cu surface is significantly smaller than that from C_6H_6 to the surface. This is fully consistent with the small $\Delta\mu=+0.06$ D for C_6H_{12}.

4. CSOV step 4: Full SCF and summary

The differences for E_{INT} and μ between the full SCF results and the CSOV step where the adsorbate orbitals are varied, $V(C_6H_6)$ and $V(C_6H_{12})$, are a measure of the nonadditivity of the decomposition of the individual CSOV contributions to the WFs and properties.[6,7] The changes in these properties are small indicating that the decomposition is additive. For the full SCF WF, the C_6H_6 interaction with Cu(111) is repulsive by −0.04 eV; this is precisely as expected since the vdW dispersion forces are not included at the HF level of theory and these forces are required to stabilize the bonding of the C_6H_6 adsorbate to the surface. However, the C_6H_{12} interaction is attractive by +0.04 eV; this is not as it should be since, again, the bond is due primarily to the vdW forces. The interaction arises from the BSSE effects that act to increase the apparent bond strength.[6,7,19] We believe that the principle BSSE error arises at the V(Cu) CSOV step, where the error will be larger for $Cu_{32}-C_6H_{12}$ than for $Cu_{32}-C_6H_{12}$. The reason for the larger BSSE-induced error in E_{INT} can be seen by comparing Figs. 3(b) and 3(e) that show the Cu polarization for C_6H_6 and C_6H_{12}, respectively. The increase of Cu charge density at the periphery of the adsorbate in the case of C_6H_6, see Fig. 3(b), is quite far from the nearest atoms of the adsorbate and even the diffuse functions added to the H atoms will not be able to help describe this polarized charge. On the other hand, for C_6H_{12}, the Cu polarization in response to the presence of the adsorbate leads, also, to increases of charge density below the first row of H atoms in C_6H_{12}. Even though the edge H atoms are 0.8 Å above the plotting plane, the diffuse basis functions on these H atoms may be able to help describe the polarized Cu charge distribution and, hence, to lead to an artificial lowering of the energy at this CSOV step. It is also understandable from Fig. 3(b) why this BSSE error for E_{INT} cannot be determined with the usual Boys-Bernardi[19] counterpoise "correction." The usual correction is made for the bare surface in the presence of the adsorbate, C_6H_6 or C_6H_{12}, basis functions. This correction will be rather small since the centers of the "ghost" adsorbate basis functions are quite far from the surface; the atoms in C_6H_6 are ~3.6 Å above the surface and the lowest row of H atoms in C_6H_{12} are still 2.7 Å above the surface; the density of a bare Cu(111) surface is rather low at these long distances from the surface. However, the polarization of the Cu charge induced by the presence of C_6H_{12} increases the Cu charge near the adsorbate, as shown by Fig. 3(e). It is this polarization, which is not taken into account in the standard Boys-Bernardi estimate of the BSSE errors, that increases the BSSE error for the adsorption of C_6H_{12} over that for the adsorption of C_6H_6.

In Fig. 4, we show the total charge-density difference plots between the full SCF density and the sum of the densities of the adsorbate and the substrate, Fig. 4(a) for C_6H_6/Cu(111) and Fig. 4(b) for C_6H_{12}/Cu(111). These total

TABLE IV. CSOV decomposition of the shifts of the high-lying C_6H_6 orbital energies due to the interaction of C_6H_6 with the Cu(111) surface as modeled with the $Cu_{32}-C_6H_6$ cluster. At the full SCF step the $1a_{2u}$ orbital is split into two cluster orbitals; see text. The projection of the gas-phase C_6H_6 orbital on the cluster is used to estimate the UPS relative intensities I of these two orbitals. All values of ε_i and $\Delta\varepsilon_i$ are given in eV.

	ε_i(free C_6H_6)	$\Delta\varepsilon_i$(FO)	$\Delta\varepsilon_i[V(\mathrm{Cu})]$	$\Delta\varepsilon_i[V(C_6H_6)]$	$\Delta\varepsilon_i$(full SCF)	$\Delta\varepsilon_i$(net)
$1a_1$	−17.46	+0.34	−0.13	−0.07	−0.02	+0.13
$1a_2$	−16.90	+0.38	−0.16	−0.10	−0.02	+0.13
1π	−16.09	+0.36	−0.14	−0.08	−0.02	+0.12
$1a_{2u}$	−13.66	+0.29	−0.16	−0.07	+0.24(40% of I)	+0.30
					−0.28(54% of I)	−0.22
$2e_{2g}$	−13.43	+0.37	−0.14	−0.08	−0.02	+0.13
$1e_{1g}$	−9.22	+0.29	−0.16	−0.07	0.00	+0.07

density differences are often used to illustrate the nature of the interaction between substrate and adsorbate, see, for example, Refs. 42 and 43. However, since these total density differences combine several distinct and different contributions to an interaction, they may be misleading and care must be taken in the analysis of these density differences.[40] The limitations of these total density difference plots is also clear from Fig. 4. For C_6H_6/Cu(111), Fig. 4(a), the Pauli exclusion principle effects and the Cu polarization shown in Figs. 3(a) and 3(b) are clear but their origin is not identified and, without the detailed data in Fig. 3, one might be tempted to associate both of these contributions with the polarization of the Cu substrate and to miss the importance of the Pauli exclusion effects. Furthermore, the weak chemisorption bond from the C_6H_6 donation to Cu clearly shown in Fig. 3(c) is not seen in Fig. 4(a) because it is swamped by the depletion of charge to satisfy the Pauli exclusion. For C_6H_{12}/Cu(111), Fig. 4(b), the changes due to the Pauli exclusion and to the Cu polarization can be seen. However, the intricacies of the polarization of the Cu substrate in response to the presence of C_6H_{12}, clearly seen in Fig. 3(e), are not seen in Fig. 4(b). Indeed, without the benefit of the decomposition of effects shown in Fig. 3, one might be tempted to view Fig. 4(b) as showing σ donation from Cu to C_6H_{12}; this would be an incorrect interpretation.

For C_6H_6/Cu(111), the major changes in the interface dipole, see Table II, are at the FO and $V(C_6H_6)$ CSOV steps and these contributions are additive to increase the interface dipole. The total change in μ is +1.4 D. For C_6H_{12}/Cu(111), the major changes in μ are at the FO and the V(Cu) CSOV steps, see Table III; furthermore, they are canceling rather than being additive. As a consequence of this cancelation, the total change in μ is only +0.7 D; this is half the increase in the interface dipole found for C_6H_6/Cu(111). The changes in the interface dipole are reflected in changes in the work function of the surface, $\Delta\phi$.[41] The measured values of $\Delta\phi$ (Ref. 41) for C_6H_6/Cu(111) and C_6H_{12}/Cu(111) are −1.05 and −0.50 eV, respectively. These values differ by a factor of 2; this is fully consistent with the factor of 2 difference in the changes of the interface-dipole moments obtained with our cluster model WFs.

V. ORBITAL ENERGIES

In Tables IV and V, we present a CSOV analysis of the orbital energies for C_6H_6 and C_6H_{12} interacting with the Cu(111) cluster, respectively. Within the framework of Koopmans' theorem, these orbital energies and, in particular, their shifts can be used to analyze photoemission spectra for adsorbates on the Cu and on other metal surfaces. [See Ref. 33 for a discussion of shifts of core-level binding energies (BEs) and Ref. 44 for a discussion of BE shifts of valence levels.] Since our concern is to interpret the BE shifts observed in ultraviolet photoemission spectroscopy (UPS) for C_6H_6 adsorbed on Cu(111) (Ref. 26) we consider only the highest valence levels derived from the free molecules with orbital energies ε in the range of ~−9.0– ~−17.5 eV. There are six such levels for C_6H_6, see Table IV, where the orbital symmetry labeling for the isolated molecule is used[45,46] to simplify comparison with experiment.[26] There are eight lev-

TABLE V. CSOV decomposition of the shifts of the high-lying C_6H_{12} orbital energies due to the interaction of C_6H_{12} with the Cu(111) surface as modeled with the $Cu_{32}-C_6H_{12}$ cluster; see the caption to Table IV.

	ε_i(free (C_6H_{12})	$\Delta\varepsilon_i$(FO)	$\Delta\varepsilon_i(V[\mathrm{Cu}])$	$\Delta\varepsilon_i(V[C_6H_{12}])$	$\Delta\varepsilon_i$(full SCF)	$\Delta\varepsilon_i$(net)
$1a_1$	−17.62	+0.34	+0.04	−0.08	+0.00	+0.30
$2a_1$	−16.43	+0.32	+0.03	−0.07	−0.00	+0.28
$1e$	−16.18	+0.32	+0.04	−0.08	−0.01	+0.28
$2e$	−14.25	+0.34	+0.04	−0.08	+0.01	+0.30
$1a_2$	−13.89	+0.36	+0.04	−0.10	0.00	+0.30
$3e$	−12.97	+0.31	+0.04	−0.07	+0.02	+0.30
$3a_1$	−12.11	+0.28	+0.04	−0.08	+0.03	+0.27
$4e$	−11.45	+0.35	+0.04	−0.09	+0.00	+0.30

els for C_6H_{12}, see Table V, and we use the C_{3v} point-group symmetry of the molecule to label these orbitals; we start the numbering as $1a_1$, $1e$, or $1a_2$, for the most deeply bound of the levels shown in Table V. For each CSOV step, we follow the occupied orbitals using, at each of the SCF iterations, the criteria of maximum overlap with the trial orbitals; this ensures that we correctly follow the molecular valence orbitals of interest. There is one important exception to this procedure. At the full SCF step for $Cu_{32}-C_6H_6$, there is, for the $1a_{2u}$ orbital, a very large mixing of the occupied C_6H_6 orbital and an orbital in the *d* band of the Cu_{32} cluster. The mixing is identified with the use of projection operator methods[47] to identify the orbitals with large adsorbate character. The mixing leads to a significant distribution of the $1a_{2u}$ UPS intensity over two orbitals and both are listed at the full SCF CSOV step along with the intensity *I* that they are expected to carry. In all other cases, the mixing of the molecular orbital with substrate orbitals was much weaker at the full SCF CSOV step and only one orbital is listed at this step. The optimized geometry for the adsorbed molecule is used for the free molecule and for all the CSOV steps. Since as noted above, geometry changes are minor, this use of a single molecular geometry for all CSOV steps will not introduce any artifacts. In both tables, the ε_i are given for the isolated adsorbate molecule and for each CSOV step, labeled as FO, $V(Cu)$, $V(C_6H_6)$, and full SCF, the $\Delta\varepsilon_i$ are given with respect to the previous step. For the FO step, the $\Delta\varepsilon_i$ are taken with respect to the values for free C_6H_6. The sign of the $\Delta\varepsilon_i$ are chosen so that $\Delta\varepsilon_i>0$ means that the values of the ε_i are larger, or closer to zero; hence $\Delta\varepsilon_i>0$ indicates that Koopmans' theorem BE is shifted toward a smaller value. The last column in Tables IV and V, labeled $\Delta\varepsilon_i$(net) gives the total change in the ε_i between the isolated adsorbate molecule and the full SCF solution for the Cu_{32}-adsorbate cluster.

For both adsorbates, at the FO step the values of the ε_i are larger, closer to zero, by between 0.28 and 0.38 eV. This increase of the ε_i arises because of the increased charge density when the Cu and adsorbate orbitals overlap and it is reasonably constant for all the orbitals of the adsorbates. For C_6H_6/Cu(111), the variation of the Cu orbitals, $V(Cu)$, leads to a small decrease in the ε_i ranging between 0.13 and 0.16 eV. This increase in the magnitude of the ε_i is because the polarization of the Cu charge acts to remove charge from the interface between adsorbate and substrate, see Fig. 4. For C_6H_{12}/Cu(111), see Table VI, the variation of the Cu orbitals, $V(Cu)$, leads to a small increase in the ε_i of $\sim$0.04 eV compared to a decrease of $\sim$0.15 eV for the $V(Cu)$ step for the case of C_6H_6/Cu(111). The increase of the ε_i for C_6H_{12} is due to the different nature of the charge redistribution of the Cu charge in the case of C_6H_{12} from that when the adsorbate is C_6H_6. Because of the open structure of C_6H_{12}, the Cu charge moves upwards into the open spaces between the lower layer of H atoms of the adsorbate. This can be seen from the charge-density difference plots and it can also be seen from the negative change of the dipole moment of the $Cu32-C_6H_{12}$ when the Cu orbitals are allowed to vary in response to presence of C_6H_{12}. The movement of the Cu charge toward the adsorbate creates an electrostatic potential that leads to an increase of the ε_i. This is the opposite of the situation at this CSOV step for C_6H_6/Cu(111) where the polarization of the Cu charge acts to remove charge from the interface between the adsorbate and substrate. The variation of the adsorbates at the $V(C_6H_6)$ and $V(C_6H_{12})$ CSOV steps lead to rather similar small increases, 0.07–0.10 eV, in the magnitudes of the ε_i. This indicates that the small π bond for C_6H_6/Cu(111) is not sufficiently strong to affect the C_6H_6 ε_i. For C_6H_6/Cu(111), the ε_i at the full SCF step are, with one important exception, rather small, ranging between 0 and −0.02 eV. The exception is the $1a_{2u}$ orbital that is split into two orbitals, as noted above, by mixing with the occupied Cu_{32} *d* band orbitals. The orbital that has 54% of the adsorbate orbital is shifted by 0.28 eV to higher BE; presumably, this orbital has bonding character between the adsorbate and substrate. The other orbital has 40% of the adsorbate $1a_{2u}$ orbital and is shifted to lower BE by 0.24 eV; presumably this orbital has antibonding character. For C_6H_{12}/Cu(111), the shifts of the full SCF orbital energies are rather small, ranging between −0.01 and +0.03 eV. This is additional evidence that the chemical interaction between the Cu surface and the adsorbed C_6H_{12} is weak. The mixing between the occupied Cu and C_6H_{12} orbitals is weak because the off-diagonal matrix elements of the Fock operator between these orbitals are small; one would expect similar small off-diagonal matrix elements involving the unoccupied orbitals at the Cu(111) surface and, hence, a small to vanishing back donation and bonding.

In the UPS studies for benzene adsorbed on a Cu(111) surface,[26] it was observed that generally all orbitals show a homogeneous shift with respect to the gas phase. One exception was the orbital $1a_{2u}$, for which a differential shift of about 0.3 eV towards higher binding energies was observed. In addition, there were significant changes reported for the position of the $1e_{1g}$ level. It has to be noted, however, that this energy level is so close to the substrate *d* states that the interpretation of the experimental data is, in fact, not unambiguous. In our calculations, the $1a_{2u}$ level splits, upon adsorption, into two components where one of the components shows a shift to higher BE, with respect to the free molecule, by 0.22 eV, see $\Delta\varepsilon_i$(net) column in Table IV. This shift could be observed in the UPS measurements as a total differential shift of 0.3 eV with respect to other C_6H_6 levels which are, on average, shifted by 0.1 eV to lower BE and it is in good agreement with the experimental data. For the UPS features that Koschel *et al.* assign to the benzene $1e_{1g}$ level, the main effect that can be seen is a broadening rather than a shift. Our cluster model results have shown that this broadening is not due to changes inherent in the adsorbed C_6H_6 molecule. We speculate about a possible origin for this broadening that is related to the presence of the Cu surface band in this energy region, a fact which is not discussed in detail in the Koschel *et al.* paper. It is possible that the apparent broadening in the $1e_{1g}$ energy region relates to scattering of Cu surface band photoelectrons by the benzene overlayer; these inelastically scattered electrons will give the appearance of intensity shifted to a higher BE. We are not aware of any experimental data for cyclohexane adsorbed on a Cu(111) surface but data for other saturated alkanes including octane adsorbed on a Cu(111) surface is available.[48] In

these data a uniform shift of all molecular levels has been observed with respect to the gas phase. This finding is in excellent agreement with the theoretical data presented here.

VI. CONCLUSIONS

In the present paper we have presented a detailed analysis of the interaction of two prototype hydrocarbons, cyclohexane and benzene, with a Cu(111) surface. Among all the low-indexed Cu surfaces, this should be the one with the weakest chemical interaction with an adsorbed molecule since the number of next nearest neighbors missing compared to the bulk only amounts to 3. In our analysis which uses a wave-function-based approach where correlation effects are treated on the MP2 level, we find that in both cases a well-defined minimum exists which allows to describe both systems as weakly adsorbed. In the case of cyclohexane, we find that the adsorption is mainly determined by the balance between the van der Waals attraction brought about by dispersion forces and the Pauli repulsion resulting from an overlap of the molecule electrons and the substrate charge density. Our results confirm previous findings in that the Pauli repulsion leads to a significant displacement of metallic charge at the surface which in turn leads to a significant lowering of the metal work function.[5] Thus we conclude that cyclohexane is physisorbed on the Cu surface. In the case of benzene, interaction energies are quite similar and also an adsorption-induced displacement of metallic charge is seen. There is also strong evidence for a small π back donation from C_6H_6 to Cu contributing to a weak chemical bond; therefore, this case is properly described as a weak chemisorption. The difference between the changes at the $V(C_6H_6)$ and the $V(C_6H_{12})$ steps provide the major part of the evidence for the chemisorption bond for C_6H_6. The changes in the interaction energy ΔE_{INT} are small and similar for both adsorbates being $\sim$25% larger for C_6H_6 than for C_6H_{12}. However, the BSSE effects could well mask small changes in ΔE_{INT}. The change in the dipole moment for C_6H_6 at this CSOV step is $\Delta\mu=+0.4$ D consistent with a back donation from adsorbate to substrate. On the other hand, at this CSOV step for C_6H_{12}, $\Delta\mu=+0.05$ D is much smaller in magnitude, consistent with the absence of back donation from C_6H_{12}. The $\Delta\rho$ at the $V(C_6H_6)$ CSOV, Fig. 3(c), step graphically shows this back donation while the $\Delta\rho$ in Fig. 3(f) graphically shows the absence of this back donation for C_6H_{12}. We have also examined the shifts of the valence level HF orbital energies ε to obtain additional confirmation of the covalent back donation bonding differences. For C_6H_{12}/Cu(111), the higher-lying C_6H_{12} ε shift uniformly at each of the CSOV steps and the shifts can be assigned to environmental, electrostatic as opposed to bonding effects. For C_6H_6/Cu(111), there is a significant difference. At the full SCF CSOV step, there is mixing of the $1a_{2u}$ benzene orbital with Cu d band orbitals, which we assign as arising from the overlap of the benzene $1a_{2u}$ orbital with the Cu d-band orbitals. The mixing of these orbitals leads to the $1a_{2u}$ C_6H_6 orbital being distributed over two $Cu_{32}-C_6H_6$ cluster orbitals. This mixing of closed-shell orbitals to form canonical HF SCF orbitals must be interpreted with caution in terms of photoelectron spectra. However, it does give direct evidence for the larger values of the off-diagonal Hamiltonian matrix elements between Cu and C_6H_6 than between Cu and C_6H_{12}. It is the similar matrix elements that drive the covalent interaction and bonding of adsorbate to substrate that, as shown above, clearly occur for C_6H_6/Cu(111) and barely, if at all, for C_6H_{12}/Cu(111). Thus the shift of the $1a_{2u}$ C_6H_6 ε provides additional evidence for an interaction that can lead to a covalent, albeit weak, chemisorption bond for C_6H_6/Cu(111).

The quantitative results of our analysis, namely, the binding energy, the change in the work function, and the frequency of the frustrated vibration normal to the surface compare very favorably with the experimental data. Altogether the results reveal that an approach using wave-function-based methods, where dispersion forces are considered on the MP2 level, has significant advantages with regard to calculations using the DFT approach since the adsorption geometry of the molecule can be obtained by an unconstrained optimization of the molecular coordinates.

ACKNOWLEDGMENTS

This work was partially supported by the National Science Foundation under Grant No. NSF CHE03-4999. We are also pleased to acknowledge partial computer support from the National Center for Supercomputing Applications, Urbana-Champaign, Illinois.

[1] N. Mott, Proc. Cambridge Philos. Soc. **34**, 568 (1938).
[2] W. Schottky, Z. Phys. **118**, 539 (1942).
[3] I. G. Hill, A. Rajagopal, and A. Kahn, Appl. Phys. Lett. **73**, 662 (1998).
[4] E. Ito, H. Oji, H. Ishii, K. Oichi, Y. Ouchi, and K. Seki, Chem. Phys. Lett. **287**, 137 (1998).
[5] P. S. Bagus, V. Staemmler, and C. Wöll, Phys. Rev. Lett. **89**, 096104 (2002).
[6] P. S. Bagus, K. Hermann, and C. W. Bauschlicher, J. Chem. Phys. **80**, 4378 (1984).
[7] P. S. Bagus and F. Illas, J. Chem. Phys. **96**, 8962 (1992).
[8] J. Hay and W. R. Wadt, J. Chem. Phys. **82**, 270 (1985).
[9] B. C. Laskowski and P. S. Bagus, Surf. Sci. **138**, 1142 (1984).
[10] B. Richter, H. Kuhlenbeck, H.-J. Freund, and P. S. Bagus, Phys. Rev. Lett. **93**, 026805 (2004).
[11] C. Wöll, K. Weiss, and P. S. Bagus, Chem. Phys. Lett. **332**, 553 (2000).
[12] C. Moller and M. S. Plesset, Phys. Rev. **46**, 618 (1934).
[13] J. A. Pople, R. Seeger, and K. Krishnan, Int. J. Quantum Chem., Symp. 11, 149 (1977).
[14] D. J. Tozer, J. S. Andrews, R. D. Amos, and N. C. Handy, Chem. Phys. Lett. **199**, 229 (1992).
[15] K. A. Fosser, R. G. Nuzzo, P. S. Bagus, and C. Wöll, J. Chem. Phys. **118**, 5115 (2003).
[16] M. A. Omary, P. Sinha, P. S. Bagus, and A. K. Wilson, J. Phys. Chem. A **109**, 690 (2005).
[17] J. L. F. DaSilva, C. Stampfl, and M. Scheffler, Phys. Rev. Lett. **90**, 066104 (2003).
[18] S. Kristyan and P. Pulay, Chem. Phys. Lett. **229**, 175 (1994).
[19] S. F. Boys and F. Bernardi, Mol. Phys. **19**, 553 (1970).
[20] T. Van Mourik, A. K. Wilson, K. A. Peterson, D. E. Woon, and T. H. Dunning, Adv. Quantum Chem. **31**, 105 (1999).
[21] H.-J. Werner, P. J. KnowlesR. D. Amos, *et al.*, MOLPRO, a package of *ab initio* programs, 2002.
[22] P. S. Bagus and C. Wöll, Chem. Phys. Lett. **294**, 599 (1998).
[23] K. A. Fosser, R. G. Nuzzo, P. S. Bagus, and C. Wöll, Angew. Chem., Int. Ed. **41**, 1735 (2002).
[24] L. Triguero, L. G. M. Petterson, B. Minaev, and H. Agren, J. Chem. Phys. **108**, 1193 (1998).
[25] A. V. Teplyakov, B. E. Bent, J. Eng, and J. G. Chen, Surf. Sci. **399**, L342 (1998).
[26] H. Koschel, G. Held, and H.-P. Steinrück, Surf. Rev. Lett. **6**, 893 (1999).

[27] The binding energy was assumed equal to the activation energy for desorption and calculated from the maximum in the TPD spectra reported for C_6H_{12} in Ref. 25 and for C_6H_6 in Ref. 26 using the Redhead formula with a preexponential factor of $\nu = 10^{13}$/s.
[28] R. P. Feynman, Phys. Rev. **56**, 340 (1939).
[29] S. A. C. McDowell, J. Comput. Chem. **18**, 1664 (1997).
[30] J. O. Hirschfelder, C. F. Curtiss, and R. B. Bird, *Molecular Theory of Gases and Liquids* (Wiley, New York, 1954).
[31] P. S. Bagus and F. Illas, Chem. Phys. Lett. **224**, 576 (1994).
[32] P. S. Bagus, C. J. Nelin, W. Müller, M. R. Philpott, and H. Seki, Phys. Rev. Lett. **58**, 559 (1987).
[33] P. S. Bagus, F. Illas, G. Pacchioni, and F. Parmigiani, J. Electron Spectrosc. Relat. Phenom. **100**, 215 (1999).
[34] C. W. Bauschlichter, P. S. Bagus, C. J. Nelin, and B. Roos, J. Chem. Phys. **85**, 354 (1986).
[35] P. S. Bagus, C. J. Nelin, K. Hermann, and M. R. Philpott, Phys. Rev. B **36**, R8169 (1987).
[36] J. L. Dunham, Phys. Rev. **41**, 721 (1932).
[37] G. Witte and C. Wöll, J. Chem. Phys. **103**, 5860 (1995).
[38] P. O. Löwdin, Phys. Rev. **97**, 1474 (1954).
[39] P. S. Bagus, K. Hermann, and C. W. Bauschlichter, J. Chem. Phys. **81**, 1966 (1984).
[40] P. S. Bagus, K. Hermann, W. Müller, and C. J. Nelin, Phys. Rev. Lett. **57**, 1496 (1986).
[41] G. Witte, S. Lukas, P. S. Bagus, and C. Wöll, Appl. Phys. Lett. (to be published).
[42] E. Wimmer, C. L. Fu, and A. J. Freeman, Phys. Rev. Lett. **55**, 2618 (1985).
[43] D. Post and E. J. Baerends, J. Chem. Phys. **78**, 5663 (1983).
[44] P. S. Bagus and K. Hermann, Appl. Surf. Sci. **22**, 444 (1985).
[45] L. Asbrink, O. Edquist, E. Lindholm, and L. E. Sedin, Chem. Phys. Lett. **5**, 192 (1970).
[46] R. Dudde, K.-H. Koch, and E.-E. Koch, Surf. Sci. **225**, 267 (1990).
[47] C. J. Nelin, P. S. Bagus, and M. R. Philpott, J. Chem. Phys. **87**, 2170 (1987).
[48] J. Weckesser, D. Fuhrmann, K. Weiss, C. Wöll, and N. V. Richardson, Surf. Rev. Lett. **4**, 209 (1997).